Asynchrony of the Early Maturation of White Matter Bundles in Healthy Infants: Quantitative Landmarks Revealed Noninvasively by Diffusion Tensor Imaging

Jessica Dubois,[1-5]* Ghislaine Dehaene-Lambertz,[2-5] Muriel Perrin,[1-5] Jean-François Mangin,[1-5] Yann Cointepas,[1-5] Edouard Duchesnay,[1-5] Denis Le Bihan,[1-5] and Lucie Hertz-Pannier[1-5]

[1]*UNAF, Service Hospitalier Frédéric Joliot, CEA, Orsay, France*
[2]*INSERM, U562, Orsay, France*
[3]*AP-HP, Radiologie Pédiatrique, Hôpital Necker-Enfants Malades, Paris, France*
[4]*INSERM, U663, Université Paris, Paris, France*
[5]*IFR49, Paris, France*

Abstract: Normal cognitive development in infants follows a well-known temporal sequence, which is assumed to be correlated with the structural maturation of underlying functional networks. Postmortem studies and, more recently, structural MR imaging studies have described qualitatively the heterogeneous spatio-temporal progression of white matter myelination. However, in vivo quantification of the maturation phases of fiber bundles is still lacking. We used noninvasive diffusion tensor MR imaging and tractography in twenty-three 1–4-month-old healthy infants to quantify the early maturation of the main cerebral fascicles. A specific maturation model, based on the respective roles of different maturational processes on the diffusion phenomena, was designed to highlight asynchronous maturation across bundles by evaluating the time-course of mean diffusivity and anisotropy changes over the considered developmental period. Using an original approach, a progression of maturation in four relative stages was determined in each tract by estimating the maturation state and speed, from the diffusion indices over the infants group compared with an adults group on one hand, and in each tract compared with the average over bundles on the other hand. Results were coherent with, and extended previous findings in 8 of 11 bundles, showing the anterior limb of the internal capsule and cingulum as the most immature, followed by the optic radiations, arcuate and inferior longitudinal fascicles, then the spinothalamic tract and fornix, and finally the corticospinal tract as the most mature bundle. Thus, this approach provides new quantitative landmarks for further noninvasive research on brain-behavior relationships during normal and abnormal development. *Hum Brain Mapp 29:14–27, 2008.*

Key words: brain; development; fascicle; fibers; myelination; tractography; MRI

INTRODUCTION

Normal cognitive development in infants follows a well-known temporal sequence, which is assumed to be correlated with the structural maturation of underlying brain functional networks. In white matter, myelin, the insulating lipid-layers wrapped around axons by oligodendrocytes, is essential for fast impulse conduction. Although myelination is only one of the numerous cerebral maturational

Contract grant sponsor: McDonnell foundation.

*Correspondence to: Jessica Dubois, Department of Radiology (CIBM), Geneva University Hospitals, Micheli-du-Crest, 24, 1211 Geneva, Switzerland. E-mail: jessica.dubois@centraliens.net

Received for publication 25 July 2006; Revised 31 October 2006; Accepted 16 November 2006

DOI: 10.1002/hbm.20363

Published online 22 February 2007 in Wiley InterScience (www.interscience.wiley.com).

postnatal processes (among which dendritic growth and synaptic overproduction in grey matter, followed by synaptic pruning), it has been shown closely related to cognitive development during the human life span [Klingberg et al., 1999; Nagy et al., 2004; Paus et al., 1999; Pujol et al., 2006; Van der Knaap et al., 1991]. Animal studies have also demonstrated such close correlations in the midbrain and spinal cord [Langworthy, 1928a,b], and neuronal activity induced by external stimulations influences the myelination process and degree [Barres and Raff, 1993; Demerens et al., 1996; Gyllensten and Malmfors, 1963; Ishibashi et al., 2006; Tauber et al., 1980].

Years ago, postmortem studies have described the asynchronous spatiotemporal progression of white matter myelination in the human brain [Brody et al., 1987; Yakovlev and Lecours, 1967]. Myelination is a long sequential nonlinear process that runs from the last trimester of gestation to at least 20 years of age, with a peak in the first postnatal year, and that progresses in an infero-superior and caudo-rostral way, from central to peripheral regions. The maturation rate depends on fiber bundles: sensory pathways become myelinated before motor pathways, projection fibers before association fibers, and occipito-parietal regions before temporo-frontal regions [Kinney et al., 1988]. However, postmortem methods preclude underlining direct relationships between structural and functional networks maturations.

By contrast, noninvasive anatomical techniques combined with cognitive assessment may allow the study of brain-behavior relationships and may be applied to the early detection of pathological development in comparison to normal landmarks. Structural magnetic resonance imaging (MRI) [Barkovich et al., 1988; Van der Knaap and Valk, 1990]; for reviews [Paus et al., 2001; Toga et al., 2006] has provided a way of studying qualitatively the biochemical modifications of the developing myelin, by showing a shortening of T1 in the "pre-myelin" state (oligodendrocyte proliferation and maturation), followed by a shortening of T2 during the "true" myelination (fibers ensheathment by oligodendroglial processes). This technique has thus confirmed the postmortem findings in the living newborns and children. In addition, sophisticated computational methods have enabled innovative investigations on the anatomo-functional correlations from childhood to adulthood [Nagy et al., 2004; Paus et al., 1999; Pujol et al., 2006; Sowell et al., 2002, 2004], but these methods are not well suited to the quantitative assessment of individuals.

Besides, diffusion tensor imaging (DTI) [for review, Le Bihan et al., 2001] has proved particularly sensitive to depict the early bundles spatial organization in newborns and infants, and explore the white matter maturation by monitoring diffusion indices that change with brain water content and myelination [Huppi et al., 1998a; Neil et al., 1998; Mukherjee et al., 2001; Partridge et al., 2004; Berman et al., 2005; Hermoye et al., 2006; Huang et al., 2006; for review Neil et al., 2002]. Recently, we have adapted a DTI fiber tractography method [for review Mori and van Zijl, 2002] to the low myelination state of infants brains, and settled an analysis of individual tracts, allowing us to demonstrate that the main bundles described in adults are already in place in the first postnatal months and providing a reliable way to study normal maturation [Dubois et al., 2006].

In the present study, our aim was to quantify the spatiotemporal sequence of DTI-tracked white matter bundles maturation in healthy infants, from 1 to 4 months of age. We designed a specific model based on the complementary information provided by diffusion indices on the respective roles of biological processes involved in white matter maturation. We then considered several commissural, projection, and associative fibers [Dubois et al. 2006], which underlie different functional systems and are known to myelinate at different time periods. Using mean diffusivity and anisotropy, the global bundles maturation was assessed by a progression in four relative stages, which took into account both the maturation state and speed of each bundle as a whole, in comparison with the average over all bundles and according to age. The modeled spatiotemporal sequence of maturation was in good agreement with, and extended postmortem and structural imaging findings. This simple approach shows promises for the quantitative study of brain-behavior relationships in normal infants, and for the early diagnostic of white matter developmental pathologies.

Working Hypotheses on the Relationships Between Maturational Processes and Diffusion Indices in the White Matter

Various indices have been shown to provide relevant information on white matter maturation [Mukherjee et al., 2002; Partridge et al., 2004]. In this study, we focused on four of them:

- mean diffusivity: $\langle D \rangle = \frac{\lambda_1+\lambda_2+\lambda_3}{3}$
- longitudinal diffusivity (along the tensor ellipsoid main axis): $\lambda_{//} = \lambda_\perp$
- transverse diffusivity (perpendicular to this axis): $\lambda_\perp = \frac{\lambda_2+\lambda_3}{2}$
- fractional anisotropy:

$$\mathrm{FA} = \sqrt{\frac{3}{2}\frac{(\lambda_1 - \langle D \rangle)^2 + (\lambda_2 - \langle D \rangle)^2 + (\lambda_3 - \langle D \rangle)^2}{\lambda_1^2 + \lambda_2^2 + \lambda_3^2}}$$

with the three diffusion tensor eigenvalues noted λ_i ($i = 1, 2, 3$; $\lambda_1 \geq \lambda_2 \geq \lambda_3$).

For the sake of simplicity, we considered three main processes that are assumed to crucially influence the diffusion indices changes during white matter development [Fig. 1, for reviews, Beaulieu et al., 2002; Neil et al., 2002].

First, progressive *fibers organization in fascicles* is likely to leave water content, membranes density and thus mean

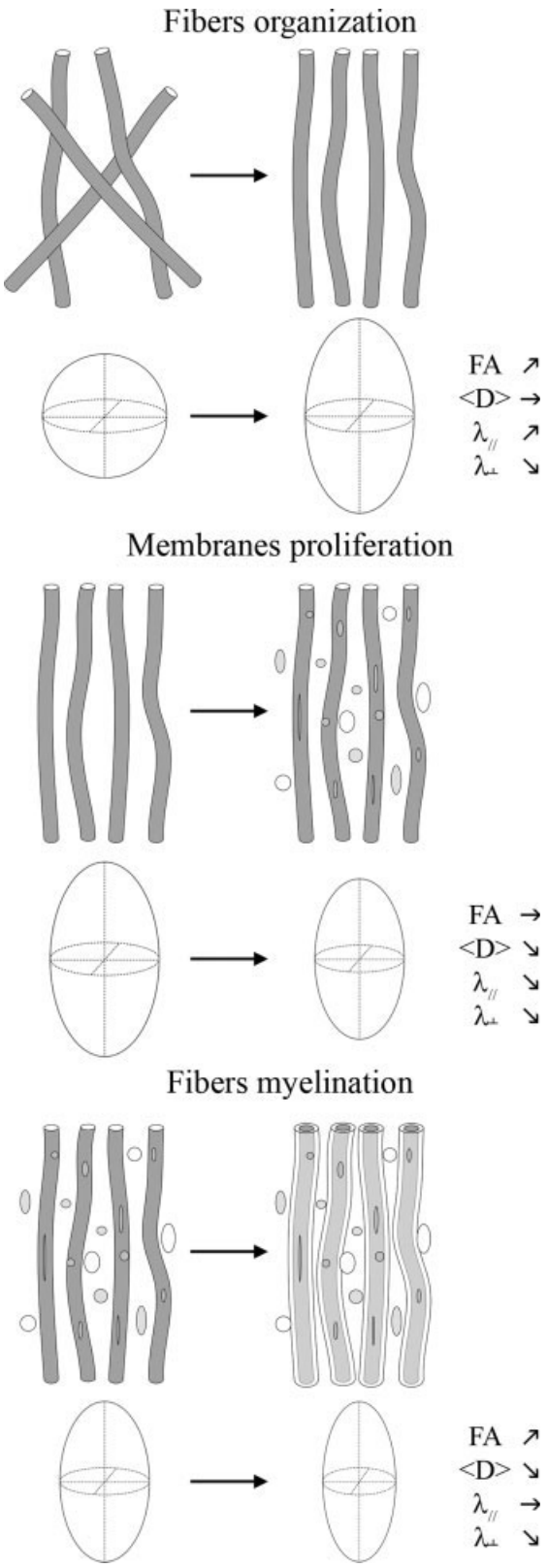

diffusivity relatively unchanged, but it may lead to an increase in anisotropy, due to increased longitudinal diffusivity and decreased transverse diffusivity (Fig. 1a), as opposed to the changes described during Wallerian degeneration [Beaulieu et al., 1996]. Progressive fibers organization is probably responsible for the anisotropy increase observed previously in unmyelinated white matter tracts of rat and rabbit pups [Drobyshevsky et al., 2005; Wimberger et al., 1995]. However, in humans, most fascicles seem to be organized during late intrauterine life [Kostovic and Jovanov-Milosevic, 2006] as fibers are to grow with the previously formed axons as guidance. Indeed, high anisotropy is already observed in poorly myelinated fascicles of premature newborns, such as the corpus callosum [Huppi et al., 1998a; Partridge et al., 2004], and the patterns of fibers tracts were found already in place in infants in our previous study, with no differences between 5 and 17 weeks [Dubois et al., 2006]. Consequently, this process was thought unlikely to contribute significantly to the expected diffusion changes over this developmental period, and, as a first approach, it was not considered further.

Second, the *proliferation and functional maturation of glial cell bodies and prolongations* (pre- and immature oligodendroglial cells and their processes, etc.) *and intracellular compartments* (cytoskeleton, etc.) are linked to a decrease in brain water content and an increase in membranes density, implying a decrease in mean diffusivity [for review Neil et al., 2002]. The first stage of myelination ("pre-myelination") is characterized by the proliferation of oligodendrocytes lineage precursors, with a decrease in water content [Prayer et al., 2001; Wimberger et al., 1995]. As this early process is rather isotropic [Baumann and Pham-Dinh, 2001], it should lead to a decrease in the three diffusivity indices, without significant change in anisotropy (Fig. 1b). Besides, both the intracellular compartments, such as neurofilaments and microtubules, and the active axonal transport do not influence anisotropy measurements [Beaulieu and Allen, 1994].

Third, the last phase of *"true" fibers myelination*, corresponding to the ensheathment of oligodendroglial processes around the axons [Van der Knaap and Valk, 1995], is accompanied by a further decrease in both membranes permeability and extracellular distance between membranes in the orthogonal direction to the fibers [for review Beaulieu, 2002]. Because of unchanged longitudinal diffusivity contrasting with decreased transverse diffusivity

Figure 1.

Hypotheses on the relationships between maturational processes and diffusion indices in the white matter. Microstructural changes at the fibers level (top) and their expected consequences on the modeled diffusion tensor (probability ellipsoid and resulting indices) (bottom) are reported during fibers organization, proliferation of membranes (glial cell bodies and prolongations, intracellular compartments, etc.) and fibers myelination.

[Gulani et al., 2001; Song et al., 2002], the anisotropy should increase while the mean diffusivity should decrease (Fig. 1c).

In summary, we hypothesized the two last processes being mainly responsible for most diffusion changes related to white matter maturation over the postnatal developmental period considered in this study (this might not be the case in younger premature newborns). Although these assumptions on indices changes might seem rather reductive in comparison with the complexity of water diffusion biophysical mechanisms in developing cerebral tissues, we thus expected that two successive steps would be observed in DTI:

- first, proliferation of "membranes" ("pre-myelination" stage), with a decrease in $\langle D \rangle$, $\lambda_{//}$ and $\lambda_{\perp}$, and without change in FA.
- second, proliferation of "membranes" and "true" fibers myelination, with both a decrease in $\langle D \rangle$, $\lambda_{//}$ and $\lambda_{\perp}$ and an increase in FA.

Consequently, we expected changes in the diffusivity indices to appear earlier than anisotropy changes in our data sets, which would provide a new and precise quantitative indicator of white matter maturation phase in infants.

MATERIALS AND METHODS

Subjects

Twenty-three healthy infants (12 boys, 11 girls) born at term (mean maturational age, i.e. corrected by gestational age at birth: 10.3 ± 3.8 weeks, range: 3.9–18.4 weeks, developmental period: 14.5 week) were included in this study after their parents gave written informed consent. Eighteen of them were included in our previous study [Dubois et al., 2006]. No sedation was used and the infants were spontaneously asleep during MR imaging. Particular precautions were taken to minimize noise exposure, by using customized headphones and covering the magnet tunnel with special noise protection foam. Six adults were also scanned (mean age: 25.6 ± 1.4 years). The study was approved by a regional ethical committee for biomedical research.

A summary of data acquisition and postprocessing is provided here as methodological issues were detailed previously [Dubois et al., 2006].

Data Acquisition

The acquisition was performed on a 1.5T MRI system (Signa LX, GEMS, USA), using a birdcage head coil. A diffusion-weighted (DW) spin-echo echo-planar technique was implemented, with a 700 s mm^{-2} b factor (TE/TR = 89.6 ms/13.8 s). A reproducible signal-to-noise ratio (32 ± 3.3) was obtained among infants by using 14–30 diffusion gradient encoding orientations [Dubois et al., 2006]. Thirty interleaved axial slices covering the whole brain were imaged, with a spatial resolution interpolated to 0.94 × 0.94 × 2.5 mm^3 at reconstruction. In adults, slice thickness was increased to 3.5 mm, and three repetitions were performed to obtain equivalent signal-to-noise ratio. Besides, conventional MR images were acquired in infants with a T2-weighted fast spin-echo sequence (TE/TR = 120/5500 ms, spatial resolution = 1.04 × 1.04 × 2 mm^3), and in adults with 3D T1-weighted spoiled gradient-echo recovery sequence (TE/TI/TR = 2.1/600/10.4 ms, spatial resolution = 0.86 × 0.86 × 1.2 mm^3).

Data Postprocessing

Data processing was performed using Anatomist [Riviere et al., 2000, http://anatomist.info] and BrainVISA softwares [Cointepas et al., 2003, http://brainvisa.info].

Image preparation

First, the DW images were corrected for the geometric distortions due to eddy currents [Mangin et al., 2002], and images were realigned in the plane of anterior/posterior commissures. Second, the diffusion tensor was estimated on a pixel-by-pixel basis and diagonalized. Maps of mean ($\langle D \rangle$), longitudinal ($\lambda_{//}$), and transverse ($\lambda_{\perp}$) diffusivities, and of fractional anisotropy (FA) were calculated.

Bundles tractography

For each infant, white matter fiber bundles were tracked in 3D using regularized particle trajectories: each particle follows locally the direction of highest diffusion, except in low anisotropy voxels resulting from fiber crossing, where the particle inertia leads to low curvature trajectory [Perrin et al., 2005]. This strategy, similar to diffusion tensor deflection [Lazar et al., 2003], overcomes simple crossing configurations, and has been validated with a phantom made up of haemodialysis fibers [Perrin et al., 2005]. It is thus particularly adapted to reconstruct the infants' immature bundles despite their low anisotropy.

Tractography "seeds" were positioned on each bundle identified on the color-coded directionality maps [Dubois et al., 2006], and twenty departure points were considered in each seed voxel. The propagation mask excluded voxels with a fractional anisotropy lower than 0.15, or a mean diffusivity higher than 2.10^{-3} mm^2 s^{-1}, which may belong to either grey matter or corticospinal fluid (CSF). The maximum curvature angle was adjusted for each bundle (15–45°), by optimizing the tract reconstruction over the infants group. The tracked fibers were selected and classified according to the regions they run through [Catani et al., 2002; Huang et al., 2004]. For infants, the bundles trajectories were assumed with a priori knowledge on the adult bundles organization [Dubois et al., 2006 for more details].

Eleven bundles were considered in the analysis (Fig. 2)

- Commissural fibers: corpus callosum (genu and splenium) (cc, ccg, ccs).

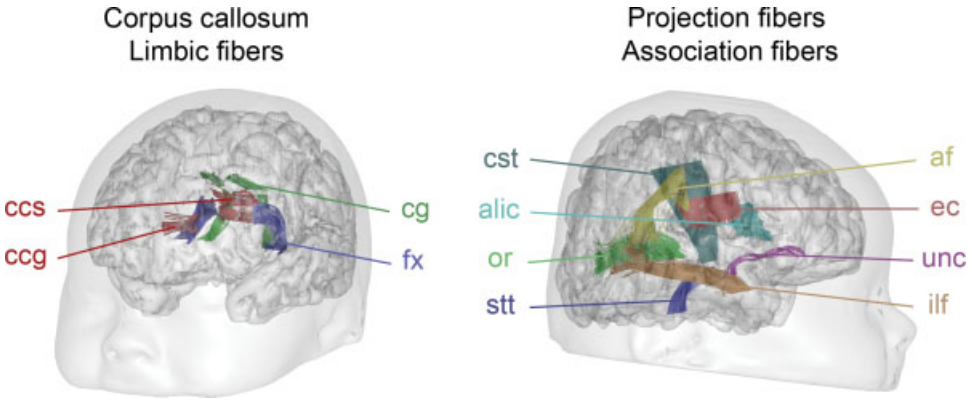

Figure 2.
Sections of the tracked bundles used for the quantification of diffusion indices. Abbreviations used: af, arcuate fasciculus; alic, anterior limb of the internal capsule; ccg and ccs, corpus callosum genu and splenium; cg, cingulum; cst, cortico-spinal tract; ec, external capsule; fx, fornix; ilf, inferior longitudinal fasciculus or optic radiations; stt, spino-thalamic tract; unc, uncinate fasciculus.

- Projection fibers: spino-thalamic tract (stt), cortico-spinal tract (cst, above the cerebral peduncles), anterior limb of the internal capsule (alic), and optic radiations (or).
- Association fibers: external capsule (ec), arcuate (af), inferior longitudinal (ilf), and uncinate (unc) fascicles.
- Limbic fibers: cingulum (cg) and fornix (fx).

Diffusion indices quantification

For the four indices ($\langle D \rangle$, $\lambda_{//}$, $\lambda_{\perp}$, FA), mean values were computed over the whole sections of the tracked bundles, which were reproducibly segmented across infants [Dubois et al., 2006; Glenn et al., 2003; Fig. 2]. In addition, the average of each index over all tracked bundles (aver) was calculated in order to characterize the white matter globally.

Quantification of White Matter Bundles Maturation

Relative maturation state, speed, and stage were then defined in each bundle to evaluate the differential maturation across bundles over the considered developmental period. As the three diffusivity indices ($\langle D \rangle$, $\lambda_{//}$, $\lambda_{\perp}$) provided redundant information in term of stages, we focused our study on both mean diffusivity ($\langle D \rangle$) and fractional anisotropy (FA).

Maturation state

We computed the median value of each index X ($X = \langle D \rangle$ or FA), over both the baby (bb) and adult (ad) groups, in each bundle (noted b) and in the average over all bundles (aver), as the indices distributions were homogeneous over the subjects group. The medians over infants were normalized by the medians over adults in order to highlight the age-related maturation effects by taking into account the geometry-based effects. To define the relative maturation *state* of each bundle, the normalized median in each bundle was then compared to the normalized median of the average over all bundles.

Consequently, the *maturation state* was defined as

$$\text{state}(b, \langle D \rangle) = 1 - \frac{M^{\text{bb}}_{\langle D \rangle}(b)/M^{\text{ad}}_{\langle D \rangle}(b)}{M^{\text{bb}}_{\langle D \rangle}(\text{aver})/M^{\text{ad}}_{\langle D \rangle}(\text{aver})}$$

$$\text{state}(b, FA) = \frac{M^{\text{bb}}_{FA}(b)/M^{\text{ad}}_{FA}(b)}{M^{\text{bb}}_{FA}(\text{aver})/M^{\text{ad}}_{FA}(\text{aver})} - 1$$

where M^{Y}_{X} is the median of X over the group Y (Y is bb, the babies, or ad, the adults), so that two possible states were considered for each index: a fascicle may be in relative *delay* (state $(b, X) < 0$) or *advance* (state $(b, X) > 0$) of maturation compared with the average over all bundles.

The statistical significance of the gap between a bundle and the average over bundles (state $(b, X) < 0$ or > 0) was confirmed using a one-sample t-test across infants ($P \leq 0.05$) for the nullity of the individual ratios

$$1 - \frac{\langle D \rangle^{\text{bb}}(b)/M^{\text{ad}}_{\langle D \rangle}(b)}{\langle D \rangle^{\text{bb}}(\text{aver})/M^{\text{ad}}_{\langle D \rangle}(\text{aver})}$$

or

$$\frac{\text{FA}^{\text{bb}}(b)/M^{\text{ad}}_{\text{FA}}(b)}{\text{FA}^{\text{bb}}(\text{aver})/M^{\text{ad}}_{\text{FA}}(\text{aver})} - 1.$$

Maturation speed

The evolution of diffusion indices with age (corrected by gestational age at birth) was clearly linear for all bundles during this period and was assessed over the infants

group by performing linear regressions. Statistically significant correlations were considered at a level of $P \leq 0.05$ after correction for multiple comparisons with false discovery rate (FDR) approach. As for the maturation state, the modeled variation magnitude of each index (over the 14.5-week developmental period) was normalized by the index median values over adults, and compared with the normalized variation of the average over bundles.

The maturation speed of the fascicle was thus computed as

$$\text{speed}(b, X) = \frac{\Delta X^{\text{bb}}(b)/M_X^{\text{ad}}(b)}{\Delta X^{\text{bb}}(\text{aver})/M_X^{\text{ad}}(\text{aver})} - 1$$

where ΔX^{bb} is the variation magnitude of the index X over the 14.5-week developmental period, so that two maturation speeds were defined for each index: a bundle may mature either slowly (speed $(b, X) < 0$) or rapidly (speed $(b, X) > 0$), relatively to the average over bundles.

Maturation stage

Finally, we assumed that the bundles maturation progresses, relatively to the average over bundles, in four stages, which combine the two distinct maturation states and speeds. In order to guarantee the progression continuity, the stages were defined from the less to the more mature (Fig. 3a):

- stage 1: the maturation state is in relative delay and the maturation speed is low
- stage 2: the state is in relative delay and the speed is high
- stage 3: the state is in relative advance and the speed is high
- stage 4: the state is in relative advance and the speed is low.

The stages were computed independently for $\langle D \rangle$ and FA.

Classification Model of White Matter Bundles Maturation

According to our working hypotheses on the relationships between maturational processes and diffusion indices, mean diffusivity changes should either occur earlier than anisotropy changes in bundles in intermediate stages, or alternatively be in equivalent stage in both the most immature and most mature bundles (see above). By combining the mean diffusivity and anisotropy stages, we thus modeled the progression of the white matter tracts maturation in five phases, from the less to the more mature one (Fig. 3b):

- phase 1: the stages of $\langle D \rangle$ and FA are equal to 1
- phase 2: the $\langle D \rangle$ stage is equal to 2 or 3, while the FA stage is equal to 1
- phase 3: the $\langle D \rangle$ and FA stages are equal to 3 and 2 respectively

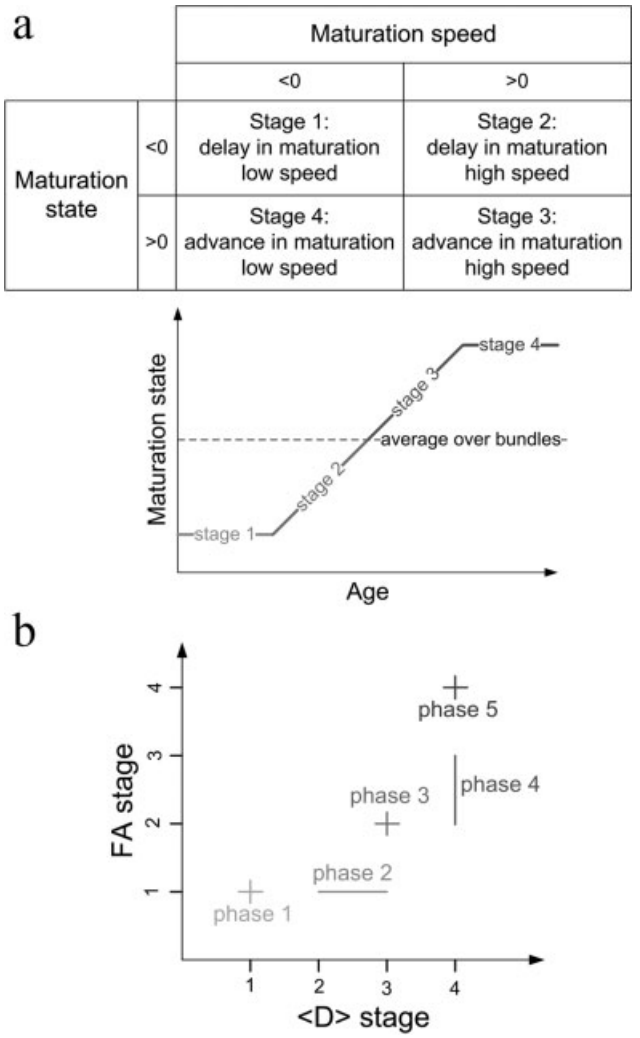

Figure 3.
Model of the progression of white matter maturation. (**a**) For <D> and FA, four maturation stages are defined according to maturation state and speed (top), and the maturation of a bundle is compared with the average over bundles (bottom). (**b**) The progression of white matter maturation is modeled in five consecutive phases, according to stages of $<D>$ and FA.

- phase 4: the $\langle D \rangle$ stage is equal to 4, whereas the FA stage is equal to 2 or 3
- phase 5: the stages of $\langle D \rangle$ and FA are equal to 4

RESULTS

Diffusion Indices Values and Age-Related Variations in Infants

Figure 4 displays the estimated medians of the diffusion indices over the infant and adult groups, for all considered

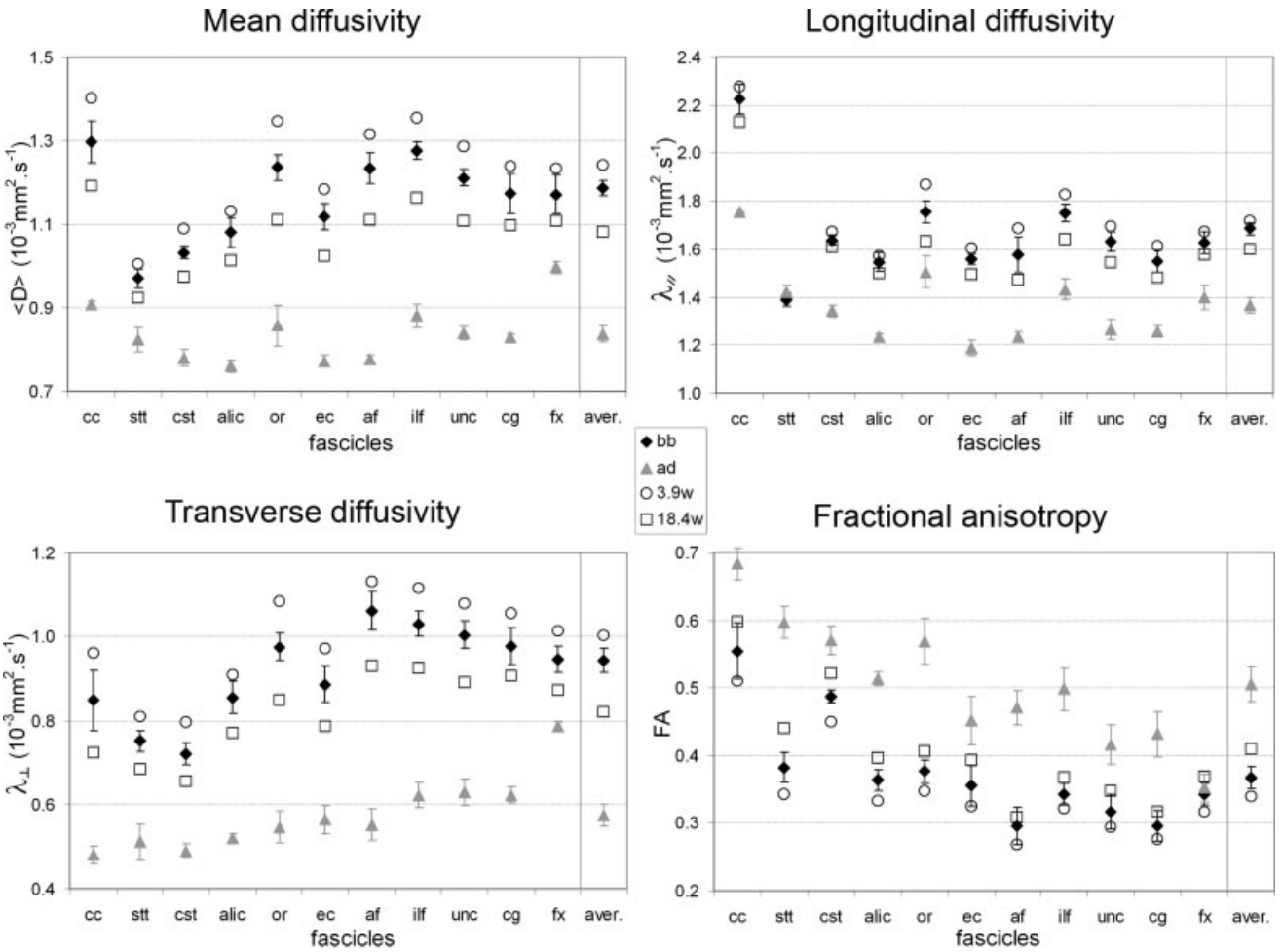

Figure 4.

Diffusion indices computed in each bundle and in the average over bundles. Medians over the babies (bb, black diamonds: age 10.3 ± 3.8 weeks) and adults (ad, gray triangles: age 25.6 ± 1.4 years) groups, with standard deviations (calculated after removing significant effects of age for infants) in plot bars, and indices, interpolated according to linear regression with age (for corrected $P \leq 0.1$), for the younger infant (white rounds: age 3.9 weeks) and the older infant (white squares: age 18.4 weeks). See Figure 2 legend for the abbreviations significance (aver: average over all bundles).

bundles. As previously reported [for review Neil et al., 2002], values of mean, longitudinal and transverse diffusivities were higher in infants than in adults, whereas anisotropy values were lower. The relative variation of fractional anisotropy among bundles was comparable in infants and adults (correlation coefficient between the groups equal to 0.79), strongly suggesting that the fibers organization in fascicles is globally similar despite incomplete maturation in infants. This observation validates our previous hypothesis for disregarding the impact of the fibers organization process on diffusion indices changes over the considered developmental period.

Age-related variations of the diffusion indices (decrease in diffusivities and increase in anisotropy) were observed over the infants group for most bundles (Table I, Fig. 5), except for the anisotropy in the corpus callosum, and for the longitudinal diffusivity in the corpus callosum, spinothalamic and cortico-spinal tracts, anterior limb of the internal capsule and fornix.

Bundles Maturation

These observations enabled us to classify the bundles along four consecutive relative stages of maturation for $\langle D \rangle$ and FA, through the evaluation of both maturation states and speeds (Fig. 6). All states were significantly different from 0. Both indices outlined the maturation asynchrony across bundles, but their respective results were different, sustaining our working hypotheses (advance of $\langle D \rangle$ stage compared with FA stage, or equivalence) in 8

TABLE I. Absolute linear changes of the diffusion indices by week of age (decrease in $\langle D \rangle$, $\lambda_{//}$, and $\lambda_{\perp}$, in 10^{-3} mm^2 s^{-1}, and increase in FA), in each bundle and in the average over bundles

	$\langle D \rangle$	$\lambda_{//}$	$\lambda_{\perp}$	FA
Corpus callosum	0.014 (0.64, *0.003*)	*ns*	0.016 (0.55, *0.009*)	*ns*
Spino-thalamic tract	0.005 (0.51, *0.008*)	*ns*	0.009 (0.69, *<0.001*)	0.007 (0.78, *<0.001*)
Cortico-spinal tract	0.008 (0.67, *0.001*)	*ns*	0.010 (0.72, *<0.001*)	0.005 (0.74, *<0.001*)
Anterior limb of the internal capsule	0.008 (0.64, *0.001*)	*ns*	0.010 (0.67, *<0.001*)	0.004 (0.56, *0.006*)
Optic radiations	0.016 (0.87, *<0.001*)	0.016 (0.80, *<0.001*)	0.016 (0.84, *<0.001*)	0.004 (0.64, *0.002*)
External capsule	0.011 (0.76, *<0.001*)	0.008 (0.50, *0.023*)	0.013 (0.77, *<0.001*)	0.005 (0.63, *0.002*)
Arcuate fasciculus	0.014 (0.79, *<0.001*)	0.015 (0.68, *0.003*)	0.014 (0.79, *<0.001*)	0.003 (0.41, *0.050*)
Inferior longitudinal fasciculus	0.013 (0.86, *<0.001*)	0.013 (0.80, *<0.001*)	0.013 (0.83, *<0.001*)	0.003 (0.57, *0.007*)
Uncinate fasciculus	0.012 (0.80, *<0.001*)	0.011 (0.64, *0.003*)	0.013 (0.78, *<0.001*)	0.004 (0.53, *0.005*)
Cingulum	0.010 (0.67, *0.001*)	0.009 (0.59, *0.006*)	0.010 (0.66, *0.001*)	0.003 (0.46, *0.022*)
Fornix	0.009 (0.67, *0.001*)	*ns*	0.010 (0.74, *<0.001*)	0.004 (0.54, *0.007*)
Average over all bundles	0.011 (0.85, *<0.001*)	0.008 (0.72, *0.004*)	0.013 (0.86, *<0.001*)	0.005 (0.80, *<0.001*)

Values inside parentheses are correlation coefficient (R) and statistical significance in italic ($P \leq 0.05$, ns: changes are not significant).

bundles over 11. These eight tracts can thus be classified according to their maturation phases (Figs 6 and 7):

- phase 1: the anterior limb of the internal capsule and the cingulum were the least mature bundles ($\langle D \rangle$/FA stage: 1/1).
- phase 2: the optic radiations, the inferior longitudinal and arcuate fascicles were relatively immature ($\langle D \rangle$/FA stage: 2/1).
- no bundle was found in phase 3.
- phase 4: the spino-thalamic tract and the fornix were more mature ($\langle D \rangle$/FA stage: 4/2 and 3).
- phase 5: the cortico-spinal tract appeared as the most mature bundle at this age ($\langle D \rangle$/FA stage: 4/4).

However, our model was not supported in three fascicles (corpus callosum, external capsule, and uncinate fasciculus) where we observed a delay of mean diffusivity compared with anisotropy.

DISCUSSION

In this study, we described quantitatively the early differential spatiotemporal maturation of white matter bundles during the first months after birth using diffusion tensor imaging and tractography. By modeling the progression of diffusion indices changes along with white matter maturation processes, we observed that the cortico-spinal tract appeared the most mature, followed by the spino-thalamic tract and the fornix, then the optic radiations, the arcuate and inferior longitudinal fascicles, and least mature were the anterior limb of the internal capsule and the cingulum. However, our model was not supported by the results in three bundles (corpus callosum, external capsule, and uncinate fasciculus).

The tractography approach provided a more precise delineation of the considered bundles than the classic regions-of-interest approach for the estimation of the diffusion indices [Dubois et al., 2006; Glenn et al., 2003; Partridge et al., 2005]. Furthermore, it allowed us to study individual tracts, contrarily to the voxel-based approach, which is not well suited to compare bundles maturation relatively to each other. Despite the low myelination of the infant's brain, we could successfully reconstruct major less-studied bundles, like the arcuate fasciculus, cingulum and fornix, and describe their maturation stages. Even though the maturation of each bundle is not spatially homogeneous [Berman et al., 2005], each tract was considered as a whole, as our aim was to compare the maturation of bundles underlying different functional systems, and not to compare the maturation of different bundles regions as described by most postmortem studies. At this point, we should remind the reader that the proposed definition of the maturation stage is not absolute, as it provided the stage of a bundle relatively to the others (for instance, a bundle in stage 4 is not necessarily fully mature, it is simply more mature than the other ones).

Maturational Processes and Diffusion Indices

We focused on two complementary diffusion indices, which are expected to reflect different biological processes during white matter maturation [Mukherjee et al., 2002; Partridge et al., 2004]. Using rather simple hypotheses, we assumed that mean diffusivity changes would reflect maturation earlier than anisotropy changes during the considered developmental period (one to four postnatal months), except in the most mature or immature bundles where equivalence would be observed. This approach was validated by experimental observations in 8 tracts out of 11, as seen on Figure 6 ($\langle D \rangle$ and FA stages), highlighting plausible biophysical relationships between postnatal maturational processes and diffusion indices changes in the white matter.

However, the model was not supported by experimental results in three tracts (corpus callosum, external capsule,

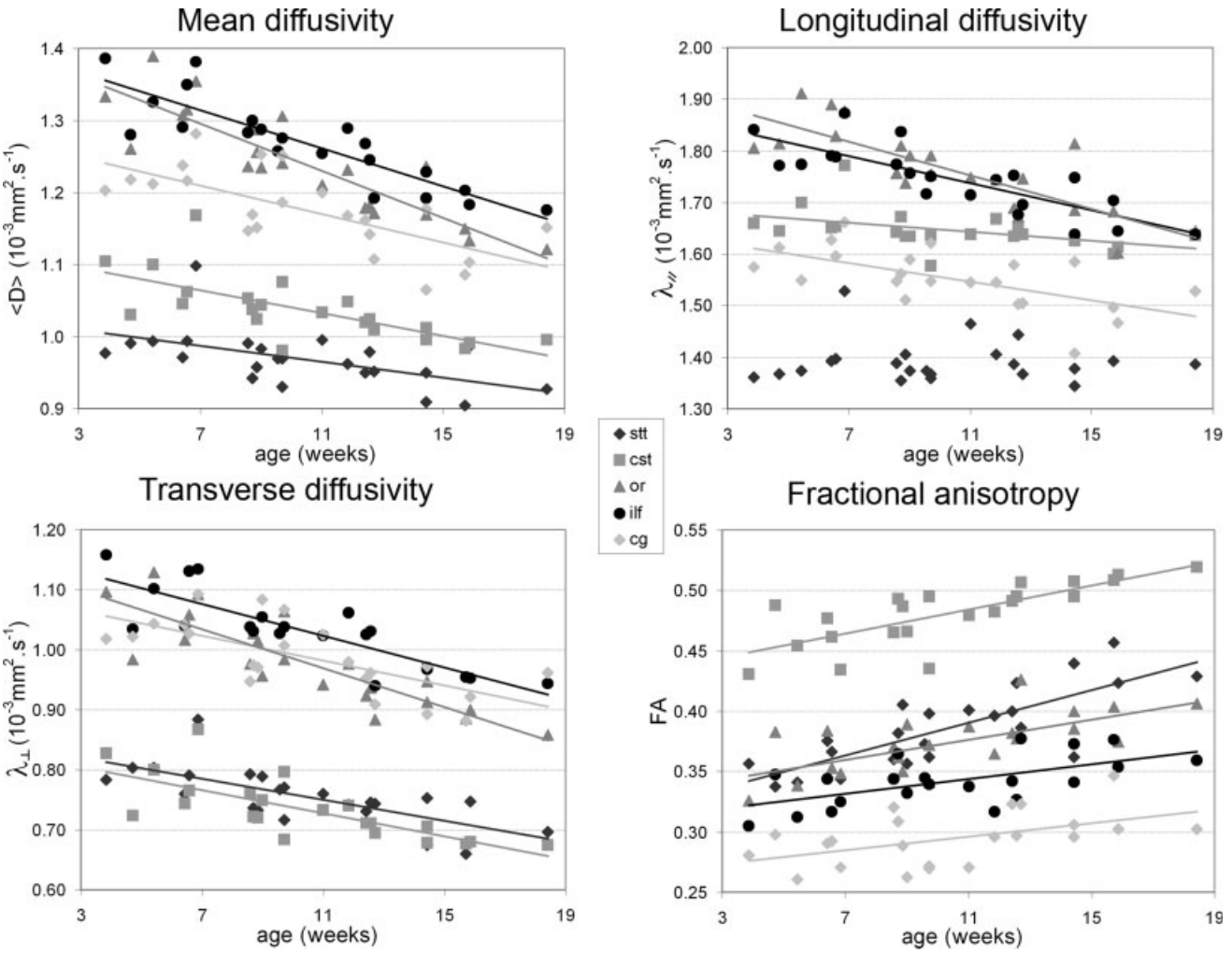

Figure 5.

Linear correlations between diffusion indices and age for examples of bundles (spino-thalamic and cortico-spinal tracts, optic radiations, inferior longitudinal fasciculus and cingulum; see Figure 2 legend for the abbreviations significance).

uncinate fasciculus), in which anisotropy stages were in advance compared with mean diffusivity stages. These three bundles were classified as stage 2 for $\langle D \rangle$, while for FA they were classified as stage 3 for the external capsule and stage 4 for both the corpus callosum and the uncinate fasciculus. Actually, this discrepancy might at least partly be related to an overestimation of the FA stages in these three bundles.

First, FA in the corpus callosum was the only measure that did not vary with age (contrarily to its mean diffusivity) suggesting that its particular geometry, with fibers tightly compact at the level of the interhemispheric fissure, may mask any other change. Its anisotropy is indeed very high in both infants and adults (Fig. 3a). Furthermore, anisotropy is already observed there in the preterm brain [Huppi et al., 1998a], whereas commissural fibers are far from being mature. Thus, the normalization by the adult values used in the calculation of the maturation state was probably insufficient to disentangle a maturation effect from organization and compactness effects.

Second, in the external capsule, FA median over the adults group may have been underestimated, as compared with the infants' one, due to crossings between the mature capsule fibers and the fanning corpus callosum fibers. By contrast, in infants, the corpus callosum is not myelinated yet, making FA measurements in the external capsule relatively robust to partial volume effects resulting from these crossings. A similar pitfall may have occurred in the uncinate fasciculus, which is located in a high crossing-fiber region.

The mean diffusivity stages would classify these three fascicles in phase 2 or 3, coherently with current knowledge

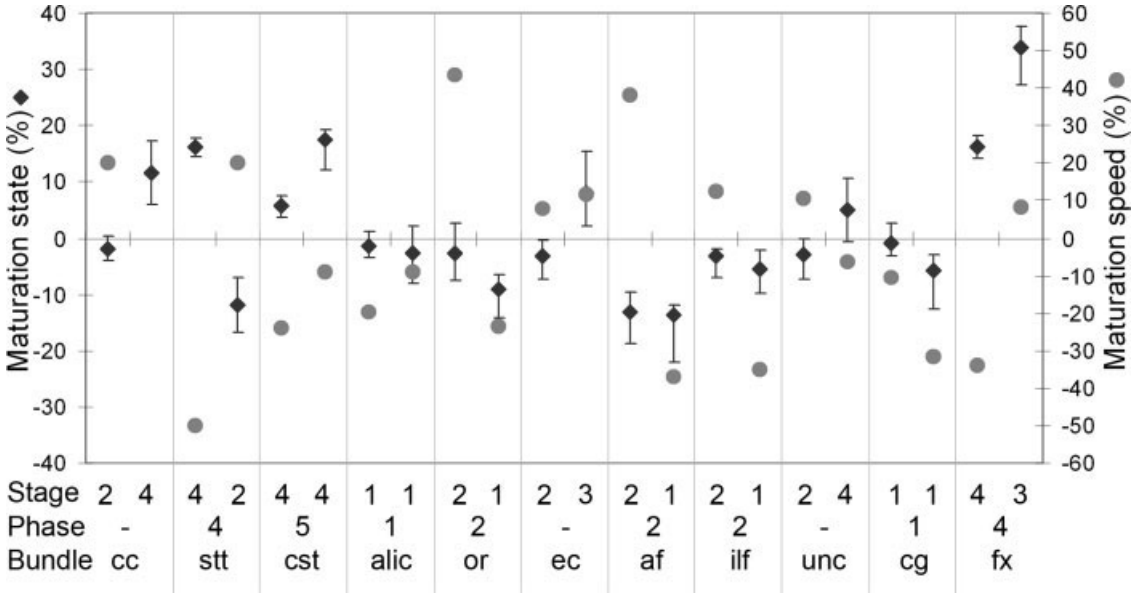

Figure 6.

Relative maturation state (black diamonds), speed (gray dots), and stage (bottom line) of each bundle for mean diffusivity (left columns) and fractional anisotropy (right columns). For maturation states, 25 and 75% quartiles of the ratio $\pm\left(\frac{X^{bb}(b)/M_X^{ad}(b)}{X^{bb}(aver)/M_X^{ad}(aver)}-1\right)$ were outlined in plot bars. The relative maturation phases, resulting from $\langle D\rangle$ and FA stages, are outlined. See Figure 2 legend for the abbreviations significance.

on these bundles myelination. However, we cannot exclude that our maturation model in phases determined through the categorization of $\langle D\rangle$ and FA stages does not take into account all underlying biophysical phenomena that modify water diffusion during the postnatal white matter maturation. Other biological processes, such as fibers organization and functional maturation, may interfere and prevent the application of this model in all bundles. Besides, Drobyshevsky and collaborators recently reported that, in the brain of rabbit pups from E22-P11 (which corresponds to a compressed and slightly different developmental time-frame, as compared with human infants), developmental changes in anisotropy coincide with the proliferation of immature oligodendrocytes before myelination [Drobyshevsky et al., 2005], whereas we assumed this process to be isotropic when isolated [Baumann and Pham-Dinh, 2001]. However, as maturation steps cannot be strictly compared across species, we believe some degree of ongoing fibers organization and compactness probably also influences their anisotropy measurements. In the corpus callosum of rabbit pups, which develops from E22 on, and where myelination begins at P11 only, the first process of our model may be predominant, with no change in mean diffusivity, decrease in transverse diffusivity, and increase in both longitudinal diffusivity and anisotropy. On the contrary, in the internal capsule where myelination begins at P5, both two first processes may be associated, with a decrease in mean, longitudinal and transverse diffusivities and increase in anisotropy. Thus, our model is coherent with animal observations, and provided meaningful results for eight fascicles of interest in infants.

Spatiotemporal Sequence of White Matter Bundles Maturation

Our in vivo approach, which highlights the bundles maturation asynchrony in healthy infants, is in good agreement with the myelination progression as determined by both postmortem [Brody et al., 1987; Kinney et al., 1988; Yakovlev and Lecours, 1967] and conventional imaging studies [for review Paus et al., 2001], which both underscore the precocity of maturation of the sensori-motor fibers relative to associative fibers. These studies report that the rostral part of the brain stem and the cerebellar peduncles are myelinated at birth (transpontine fibers, spino-thalamic tract, and cortical spinal tract). In the telencephalon, myelination begins in the posterior limb of the internal capsule during the third trimester of gestation, followed by the acoustic and optic radiations at birth, the rolandic area around 4 months, the external capsule around 10 months, and the frontal white matter by 1 year of age. The latest areas to start their myelination are the associative parietal and temporal areas (connected by

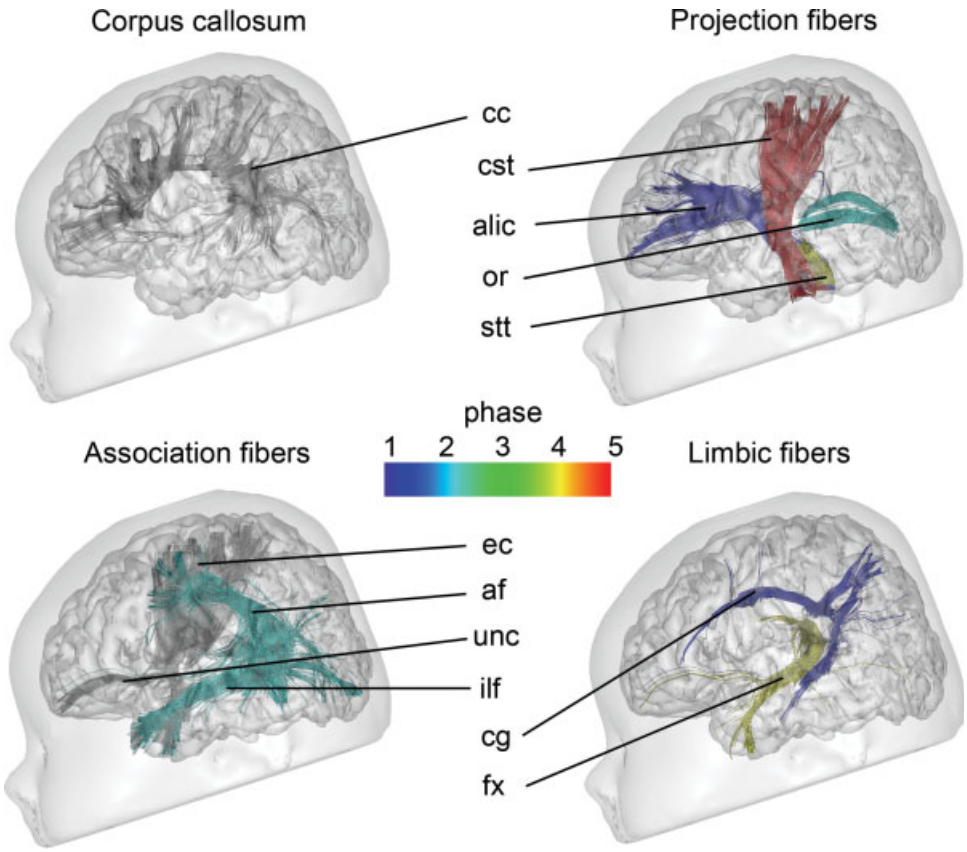

Figure 7.
Relative maturation phases of all reconstructed tracts (from Fig. 6; from blue to red: phases 1 to 5; in grey: tracts whose results are contradictory to the model). See Figure 2 legend for the abbreviations significance.

arcuate and longitudinal fasciculi) with a protracted course up to adulthood [Paus et al., 1999]. The corpus callosum myelinates progressively from birth on, according to the maturation of the regions of origin of the cortico-cortical crossing fibers.

Furthermore, our infant's data on individual bundles extend previous knowledge, by showing dissociations within a functional system. In the limbic system for example, the fornix is in advance relative to the cingulum. This observation could be related to differences in the phylogenetic origins of the bundles [Mega et al., 1997]: the fornix is a relatively old structure, whereas the cingulum has appeared in the most evolved mammals. Fornix, which is to be involved in memory and associative learnings [Brasted et al., 2003; Eacott and Gaffan, 2005], is identified in vitro by 10 weeks of gestation [Rados et al., 2006]. Actually, behavioral experiments using non nutritive sucking may be based on its relative maturation in newborns, even born preterm [Dehaene-Lambertz, 1997], as they rely on conditional learning between stimulus presentation and sucking behavior.

Model Methodological Issues and Limitations

One of the major advantages of our approach is its non-invasive application in living healthy infants, to determine the normal asynchronous bundles maturation, thus giving the possibility to correlate these microstructural observations with functional and behavioral results. Knowledge based on postmortem studies is intrinsically limited as the brain "normal" development of dead subjects may be questionable because of incorrect diagnostic, undetected metabolic troubles, insufficient or even painful stimulation in sick infants, etc. that could interfere with normal cerebral maturation, and precise corresponding functional assessment cannot be obtained.

Nevertheless, some methodological issues and limitations of this study should be kept in mind. The classification model was implemented over a short range of age after birth (1–4-month-old infants), as we did not succeed to reliably image older healthy infants without sedation. Our model is valid only when maturation changes are ongoing, as all states and speeds become equal to 0 when the adult pattern is reached (all bundles are then in the same relative stage as the average over bundles). Because we were working over a restricted developmental period during which maturational changes are intense, we assumed a continuous and linear progression of maturation, without plateau in the slope of the curve. However, this type of model might be less accurate for the study of later development [Mukherjee and McKinstry, 2006].

The maturation stages were defined according to maturation states and speeds, which were computed by comparing infants and adults data. To do so, DTI acquisition parameters were adapted in adults in order to keep equivalent signal-to-noise ratio and relatively identical partial volume effects through the slice in both groups. Nevertheless, the in-plane spatial resolution and the b factor were kept the same, despite differing diffusivity properties.

By principle, fibers reconstructed with the trajectory regularization algorithm are to include more places with crossing fibers than linear algorithms like FACT [Mori et al., 1999], which may be problematic for the indices quantification on average over the tract, as previously mentioned for the external capsule. We could have excluded these regions from the analysis, by discarding voxels with low FA, but this would have introduced a systematic bias in the quantitative analysis of bundles maturation, with an uncertainty on the location of suppressed voxels.

As a reference to assess the relative differential bundles maturation, the averages of the diffusion indices were calculated over all tracked bundles, instead of over the whole white matter because, in the infant brain, tissue segmentation would require the acquisition of complementary T1 and T2 weighted images [Huppi et al., 1998b], and its accuracy is limited due to the small contrast difference between white and grey matter.

CONCLUSION

By imaging the brain of healthy infants with diffusion tensor imaging and tractography, we were able to highlight both noninvasively and quantitatively relative spatiotemporal differences of the early maturation of white matter bundles. The designed relative maturation stages confirmed and extended postmortem knowledge, showing the anterior limb of the internal capsule and the cingulum being the most immature, followed by the optic radiations, the arcuate and inferior longitudinal fascicles, then the spino-thalamic tract and the fornix, and finally the corticospinal tract as the most mature bundle. Such an approach offers great opportunities for the investigation of the relationships between the maturation of structural connectivity and the normal functional development in humans. It also provides useful landmarks for the future demonstration of pathological cognitive development in early infancy.

ACKNOWLEDGMENTS

The authors thank Cyril Poupon, Franck Lethimonnier, Denis Rivière, and Arnaud Cachia for support on DTI acquisition and postprocessings, Mr Brunet from Ravier-Touzard Company for designing a baby bouncer chair specifically adapted to the head coil, and Pr Brunelle for the MRI access.

REFERENCES

Barkovich AJ, Kjos BO, Jackson DE Jr, Norman D (1988): Normal maturation of the neonatal and infant brain: MR imaging at 1.5 T. Radiology 166:173–180.

Barres BA, Raff MC (1993): Proliferation of oligodendrocyte precursor cells depends on electrical activity in axons. Nature 361:258–260.

Baumann N, Pham-Dinh D (2001): Biology of oligodendrocyte and myelin in the mammalian central nervous system. Physiol Rev 81:871–927.

Beaulieu C (2002): The basis of anisotropic water diffusion in the nervous system—a technical review. NMR Biomed 15:435–455.

Beaulieu C, Allen PS (1994): Determinants of anisotropic water diffusion in nerves. Magn Reson Med 31:394–400.

Beaulieu C, Does MD, Snyder RE, Allen PS (1996): Changes in water diffusion due to Wallerian degeneration in peripheral nerve. Magn Reson Med 36:627–631.

Berman JI, Mukherjee P, Partridge SC, Miller SP, Ferriero DM, Barkovich AJ, Vigneron DB, Henry RG (2005): Quantitative diffusion tensor MRI fiber tractography of sensorimotor white matter development in premature infants. NeuroImage 27:862–871.

Brasted PJ, Bussey TJ, Murray EA, Wise SP (2003): Role of the hippocampal system in associative learning beyond the spatial domain. Brain 126:1202–1223.

Brody BA, Kinney HC, Kloman AS, Gilles FH (1987): Sequence of central nervous system myelination in human infancy. I. An autopsy study of myelination. J Neuropathol Exp Neurol 46:283–301.

Catani M, Howard RJ, Pajevic S, Jones DK (2002): Virtual in vivo interactive dissection of white matter fasciculi in the human brain. NeuroImage 17:77–94.

Cointepas Y, Poupon C, Maroy R, Riviere D, Le Bihan D, Mangin JF (2003): A freely available Anatomist/Brainvisa package for analysis of diffusion MR data. NeuroImage 19:S810. Proceedings of the 9th HBM Scientific Meeting, New York, USA.

Dehaene-Lambertz G (1997): Assessment of perinatal pathologies in premature neonates using a syllable discrimination task. Biol Neonate 71:299–305.

Demerens C, Stankoff B, Logak M, Anglade P, Allinquant B, Couraud F, Zalc B, Lubetzki C (1996): Induction of myelination in the central nervous system by electrical activity. Proc Natl Acad Sci USA 93:9887–9892.

Drobyshevsky A, Song SK, Gamkrelidze G, Wyrwicz AM, Derrick M, Meng F, Li L, Ji X, Trommer B, Beardsley DJ, Luo NL, Back SA, Tan S (2005): Developmental changes in diffusion anisotropy coincide with immature oligodendrocyte progression and maturation of compound action potential. J Neurosci 25:5988–5997.

Dubois J, Hertz-Pannier L, Dehaene-Lambertz G, Cointepas Y, Le Bihan D (2006): Assessment of the early organization and maturation of infants' cerebral white matter fiber bundles: A feasibility study using quantitative diffusion tensor imaging and tractography. NeuroImage 30:1121–1132.

Eacott MJ, Gaffan EA (2005): The roles of perirhinal cortex, postrhinal cortex, and the fornix in memory for objects, contexts, and events in the rat. Q J Exp Psychol B 58:202–217.

Glenn OA, Henry RG, Berman JI, Chang PC, Miller SP, Vigneron DB, Barkovich AJ (2003): DTI-based three-dimensional tractography detects differences in the pyramidal tracts of infants and children with congenital hemiparesis. J Magn Reson Imaging 18:641–648.

Gulani V, Webb AG, Duncan ID, Lauterbur PC (2001): Apparent diffusion tensor measurements in myelin-deficient rat spinal cords. Magn Reson Med 45:191–195.

Gyllensten L, Malmfors T (1963): Myelinization of the optic nerve and its dependence on visual function—A quantitative investigation in mice. J Embryol Exp Morphol 11:255–266.

Hermoye L, Saint-Martin C, Cosnard G, Lee SK, Kim J, Nassogne MC, Menten R, Clapuyt P, Donohue PK, Hua K, Wakana S, Jiang H, van Zijl PC, Mori S (2006): Pediatric diffusion tensor imaging: Normal database and observation of the white matter maturation in early childhood. NeuroImage 29:493–504.

Huang H, Zhang J, van Zijl PC, Mori S (2004): Analysis of noise effects on DTI-based tractography using the brute-force and multi-ROI approach. Magn Reson Med 52:559–565.

Huang H, Zhang J, Wakana S, Zhang W, Ren T, Richards LJ, Yarowsky P, Donohue P, Graham E, van Zijl PC, Mori S (2006): White and gray matter development in human fetal, newborn and pediatric brains. Neuroimage 33:27–38.

Huppi PS, Maier SE, Peled S, Zientara GP, Barnes PD, Jolesz FA, Volpe JJ (1998a): Microstructural development of human newborn cerebral white matter assessed in vivo by diffusion tensor magnetic resonance imaging. Pediatr Res 44:584–590.

Huppi PS, Warfield S, Kikinis R, Barnes PD, Zientara GP, Jolesz FA, Tsudi MK, Volpe JJ (1998b): Quantitative magnetic resonance imaging of brain development in premature and mature newborns. Ann Neurol 43:224–235.

Ishibashi T, Dakin KA, Stevens B, Lee PR, Kozlov SV, Stewart CL, Fields RD (2006): Astrocytes promote myelination in response to electrical impulses. Neuron 49:823–832.

Kinney HC, Brody BA, Kloman AS, Gilles FH (1988): Sequence of central nervous system myelination in human infancy. II. Patterns of myelination in autopsied infants. J Neuropathol Exp Neurol 47:217–234.

Klingberg T, Vaidya CJ, Gabrieli JD, Moseley ME, Hedehus M (1999): Myelination and organization of the frontal white matter in children: A diffusion tensor MRI study. Neuroreport 10: 2817–2821.

Kostovic I, Jovanov-Milosevic N (2006): The development of cerebral connections during the first 20–45 weeks' gestation. Semin Fetal Neonatal Med 11:415–422.

Langworthy OR (1928a): A correlated study of the development of reflex activity in fetal and young kittens and the myelinization of the tracts in the nervous system. Contrib Embryol 20:127–172.

Langworthy OR (1928b): The behaviour of pouch young opossums correlated with the myelinization of tracts in the central nervous system. J Comp Neurol 46:201–248.

Lazar M, Weinstein DM, Tsuruda JS, Hasan KM, Arfanakis K, Meyerand ME, Badie B, Rowley HA, Haughton V, Field A, Alexander AL (2003): White matter tractography using diffusion tensor deflection. Hum Brain Mapp 18:306–321.

Le Bihan D, Mangin JF, Poupon C, Clark CA, Pappata S, Molko N, Chabriat H (2001): Diffusion tensor imaging: Concepts and applications. J Magn Reson Imaging 13:534–546.

Mangin JF, Poupon C, Clark C, Le Bihan D, Bloch I (2002): Distortion correction and robust tensor estimation for MR diffusion imaging. Med Image Anal 6:191–198.

Mega MS, Cummings JL, Salloway S, Malloy P (1997): The limbic system: An anatomic, phylogenetic, and clinical perspective. J Neuropsychiatry Clin Neurosci 9:315–330.

Mori S, Crain BJ, Chacko VP, van Zijl PC (1999): Three-dimensional tracking of axonal projections in the brain by magnetic resonance imaging. Ann Neurol 45:265–269.

Mori S, van Zijl PC (2002): Fiber tracking: Principles and strategies—A technical review. NMR Biomed 15:468–480.

Mukherjee P, McKinstry RC (2006): Diffusion tensor imaging and tractography of human brain development. Neuroimaging Clin N Am 16:19–43.

Mukherjee P, Miller JH, Shimony JS, Conturo TE, Lee BC, Almli CR, McKinstry RC (2001): Normal brain maturation during childhood: Developmental trends characterized with diffusion-tensor MR imaging. Radiology 221:349–358.

Mukherjee P, Miller JH, Shimony JS, Philip JV, Nehra D, Snyder AZ, Conturo TE, Neil JJ, McKinstry RC (2002): Diffusion-tensor MR imaging of gray and white matter development during normal human brain maturation. Am J Neuroradiol 23:1445–1456.

Nagy Z, Westerberg H, Klingberg T (2004): Maturation of white matter is associated with the development of cognitive functions during childhood. J Cogn Neurosci 16:1227–1233.

Neil JJ, Shiran SI, McKinstry RC, Schefft GL, Snyder AZ, Almli CR, Akbudak E, Aronovitz JA, Miller JP, Lee BC, Conturo TE (1998): Normal brain in human newborns: Apparent diffusion coefficient and diffusion anisotropy measured by using diffusion tensor MR imaging. Radiology 15:57–66.

Neil JJ, Miller J, Mukherjee P, Hüppi PS (2002): Diffusion tensor imaging of normal and injured developing human brain—A technical review. NMR Biomed 15:543–552.

Partridge SC, Mukherjee P, Henry RG, Miller SP, Berman JI, Jin H, Lu Y, Glenn OA, Ferriero DM, Barkovich AJ, Vigneron DB (2004): Diffusion tensor imaging: Serial quantitation of white matter tract maturity in premature newborns. NeuroImage 22: 1302–1314.

Partridge SC, Mukherjee P, Berman JI, Henry RG, Miller SP, Lu Y, Glenn OA, Ferriero DM, Barkovich AJ, Vigneron DB (2005): Tractography-based quantitation of diffusion tensor imaging parameters in white matter tracts of preterm newborns. J Magn Reson Imaging 22:467–474.

Paus T, Zijdenbos A, Worsley K, Collins DL, Blumenthal J, Giedd JN, Rapoport JL, Evans AC (1999): Structural maturation of neural pathways in children and adolescents: In vivo study. Science 283:1908–1911.

Paus T, Collins DL, Evans AC, Leonard G, Pike B, Zijdenbos A (2001): Maturation of white matter in the human brain: A review of magnetic resonance studies. Brain Res Bull 54:255–266.

Perrin M, Poupon C, Cointepas Y, Rieul B, Golestani N, Pallier C, Riviere D, Constantinesco A, Le Bihan D, Mangin JF (2005): Fiber tracking in q-ball fields using regularized particle trajectories. Proceedings of the IPMI Scientific Meeting, Glenwood Springs, USA, LNCS-3565:52–63.

Prayer D, Barkovich AJ, Kirschner DA, Prayer LM, Roberts TP, Kucharczyk J, Moseley ME (2001): Visualization of nonstructural changes in early white matter development on diffusion-weighted MR images: Evidence supporting premyelination anisotropy. Am J Neuroradiol 22:1572–1576.

Pujol J, Soriano-Mas C, Ortiz H, Sebastian-Galles N, Losilla JM, Deus J (2006): Myelination of language-related areas in the developing brain. Neurology 66:339–343.

Rados M, Judas M, Kostovic I (2006): In vitro MRI of brain development. Eur J Radiol 57:187–198.

Riviere D, Papadopoulos-Orfanos D, Poupon C, Poupon F, Coulon O, Poline JB, Frouin V, Regis J, Mangin JF (2000): A structural browser for human brain mapping. NeuroImage 11:S912. Proceedings of the 6th HBM Scientific Meeting, San Antonio, USA.

Song SK, Sun SW, Ramsbottom MJ, Chang C, Russell J, Cross AH (2002): Dysmyelination revealed through MRI as increased radial (but unchanged axial) diffusion of water. NeuroImage 17: 1429–1436.

Sowell ER, Trauner DA, Gamst A, Jernigan TL (2002): Development of cortical and subcortical brain structures in childhood and adolescence: A structural MRI study. Dev Med Child Neurol 44:4–16.

Sowell ER, Thompson PM, Leonard CM, Welcome SE, Kan E, Toga AW (2004): Longitudinal mapping of cortical thickness and brain growth in normal children. J Neurosci 24:8223–8231.

Tauber H, Waehneldt TV, Neuhoff V (1980): Myelination in rabbit optic nerves is accelerated by artificial eye opening. Neurosci Lett 16:235–238.

Toga AW, Thompson PM, Sowell ER (2006): Mapping brain maturation. Trends Neurosci 29:148–159.

Van der Knaap MS, Valk J (1990): MR imaging of the various stages of normal myelination during the first year of life. Neuroradiology 31:459–470.

Van der Knaap MS, Valk J (1995): Myelin and white matter. In: Van der Knaap MS, Valk J, editors. Magnetic Resonance of Myelin, Myelination and Myelin Disorders. Berlin: Springer-Verlag. pp 1–17.

Van der Knaap MS, Valk J, Bakker CJ, Schooneveld M, Faber JA, Willemse J, Gooskens RH (1991): Myelination as an expression of the functional maturity of the brain. Dev Med Child Neurol 33:849–857.

Wimberger DM, Roberts TP, Barkovich AJ, Prayer LM, Moseley ME, Kucharczyk J (1995): Identification of premyelination by diffusion-weighted MRI. J Comput Assist Tomogr 19:28–33.

Yakovlev PI, Lecours AR (1967): The myelogenetic cycles of regional maturation in the brain. In: Minowski A. editor. Regional Development of the Brain in Early Life. Oxford: Blackwell. pp 3–69.